

plated nucleotide addition to the 3' end of amplified products by Taq DNA polymerase, enabling reliable identification of 1-base pair alleles present in 7.4% of the markers [M. J. Brownstein, J. D. Carpten, J. R. Smith, *Biotechniques* **20**, 1004 (1996)]. We obtained 97.1% of data sought with survey markers. Blinded duplicate typing of 7560 alleles provided a genotyping error rate estimate of 0.26%. The observed rate of non-Mendelian inheritance was  $7.06 \times 10^{-4}$ .

15. In the model used, affected men were assumed to be carriers of a rare autosomal dominant gene frequency  $q = 0.003$  (6), with a fixed 15% phenocopy rate, while all unaffected men under 75 and all women were assumed to be of unknown phenotype. In men over age 75, the lifetime penetrance of gene-carriers was estimated to be 63% (based on a population based segregation analysis performed by H.G., in preparation, and the lifetime risk of prostate cancer for non-carriers was 16% in this age class (based on SEER data) [C. L. Kosary, L. A. G. Ries, B. A. Miller, B. F. Hankey, A. Harras, B. K. Edwards (Eds.), *SEER Cancer Statistics Review, 1973-1992: Tables and Graphs*, National Cancer Institute, NIH Pub. No. 96-2789, Bethesda, MD, 1995]. This is a conservative model as it minimizes the chances of incorrectly assuming that a young unaffected male is a noncarrier. The fact that nonparametric methods produce results of similar statistical significance (Table 2) adds confidence to the conclusion that the observed linkage is not strongly dependent on the choice of this particular model.
16. Standard parametric likelihood analysis was performed by means of FASTLINK [R. W. Cottingham Jr., R. M. Idury, A. A. Schaffer, *Am. J. Hum. Genet.* **53**, 252 (1993)] for two-point linkage and VITESSE [J. R. O'Connell and D. E. Weeks, *Nature Genet.* **11**, 402 (1995)] for multipoint linkage analysis. Multipoint analysis has the advantage of utilizing data from multiple linked markers to maximize the information in a given pedigree. Nonparametric multipoint analysis, which is robust even when the mode of inheritance is not known, was also performed, with GENEHUNTER [L. Kruglayk and E. S. Lander, *Am. J. Hum. Genet.* **57**, 439 (1995)] to calculate normalized Z scores and associated P values. In all of the linkage analyses, allele frequencies for the markers were estimated from independent individuals in the families and unrelated individuals separately for the North American and Swedish families. CRIMAP [E. S. Lander and P. Green, *Proc. Natl. Acad. Sci. U.S.A.* **84**, 2363 (1987)] was used to order the multiple markers on chromosome 1 using the genotype data from all pedigrees. The BUILD option of CRIMAP was first used to establish the order of markers with at least a likelihood ratio of 1000:1. The FLIP option was then used to calculate the likelihood of alternative marker orders by permuting adjacent loci (five flanking markers). The most likely order thus determined is the same as the published order (<http://cedar.soton.ac.uk/pub>). The admixture test as implemented in HOMOG [J. Ott, *Analysis of Human Genetic Linkage* (Johns Hopkins Univ. Press, Baltimore, 1985), pp. 200-203] was used to test for genetic heterogeneity in the context of the two-point parametric analysis.
17. The evaluation of age as a variable is confounded because of the changing methods used to diagnose this disease, and increased interest in screening for this disease. For the years prior to the use of prostate-specific antigen (PSA), diagnosis of prostate cancer was often not made until men presented with advanced disease, whereas today most men are diagnosed younger and at an earlier stage.
18. The expert technical assistance of C. Ewing and J. Robinson, and the help of X. Chen, D. Schwengel, R. Paul, C. Engstrand, A. Kallioniemi, L. Hardie, and B. Carter during the early phases of this work is acknowledged. We also thank B. Childs, J. Isaacs, and D. Coffey for helpful advice. We acknowledge the assistance of L. Middleton, C. Francomano, and the Family Studies Core of the National Center for Human Genome Research (NCHGR), and the Genetic Resources Core Facility (JHU). We also acknowledge A. Lowe and D. Gilbert at the Applied Biosystems Division of Perkin-Elmer for providing valuable

genotyping technical support. We wish to thank all the physicians who referred families for this study. Supported by grants from U.S. Public Health Service SPORE CA58236; The Fund for Research and Progress in Urology; The Johns Hopkins University; Swedish Cancer Society (Cancerfonden); Lion's

Cancer Foundation, Department of Oncology, Umeå Universitet, and a 1995 CaPCURE award. D.F. is supported by a grant from American Foundation for Urologic Disease.

1 October 1996; accepted 24 October 1996

## RAC Regulation of Actin Polymerization and Proliferation by a Pathway Distinct from Jun Kinase

Tom Joneson,\* Michele McDonough,\* Dafna Bar-Sagi, Linda Van Aelst†

The RAC guanine nucleotide binding proteins regulate multiple biological activities, including actin polymerization, activation of the Jun kinase (JNK) cascade, and cell proliferation. RAC effector loop mutants were identified that separate the ability of RAC to interact with different downstream effectors. One mutant of activated human RAC protein, RAC<sup>V12H40</sup> (with valine and histidine substituted at position 12 and 40, respectively), was defective in binding to PAK3, a Ste20-related p21-activated kinase (PAK), but bound to POR1, a RAC-binding protein. This mutant failed to stimulate PAK and JNK activity but still induced membrane ruffling and mediated transformation. A second mutant, RAC<sup>V12L37</sup> (with leucine substituted at position 37), which bound PAK but not POR1, induced JNK activation but was defective in inducing membrane ruffling and transformation. These results indicate that the effects of RAC on the JNK cascade and on actin polymerization and cell proliferation are mediated by distinct effector pathways that diverge at the level of RAC itself.

The RAC proteins have been implicated in the regulation of various fundamental cellular processes including actin cytoskeletal organization (1), transcriptional activation (2), and cell proliferation (3-5). To identify the effector pathways that mediate the biological activities induced by RAC, we isolated mutant RAC proteins that could discriminate among the RAC targets PAK and POR1 in the yeast two-hybrid system. PAK proteins are a family of highly conserved serine-threonine kinases that are activated by direct interaction with RAC1 (6). A role for PAK has been suggested in mediating RAC-induced activation of JNK and p38 mitogen-activated protein (MAP) kinase cascades (7). POR1 interacts with RAC1 and appears to function in RAC-induced membrane ruffling (8).

Libraries of vectors expressing mutant human RAC proteins fused to the LexA DNA binding domain (LBD) were created by polymerase chain reaction (PCR) mutagenesis (9) and screened for interaction with PAK3 and POR1. Two mutants con-

taining a single amino acid substitution in the RAC effector loop were identified. One mutant, RAC<sup>V12H40</sup>, failed to bind PAK3 but did bind POR1, and another mutant, RAC<sup>V12L37</sup>, bound PAK3 but not POR1 (Table 1). Identical binding profiles were obtained for the interaction of these mutants with PAK1 (10).

To investigate the biological activities of the RAC mutants, we first examined their abilities to stimulate PAK and activate the JNK pathway. COS-1 cells were cotransfected with either RAC<sup>V12</sup>, RAC<sup>V12H40</sup>, or RAC<sup>V12L37</sup> expression plasmids and a plasmid encoding a Myc-tagged version of PAK1. PAK1 activity was assayed in immunoprecipitates with myelin basic protein (MBP) as the substrate (11). Expression of RAC<sup>V12L37</sup> resulted in stimulation of PAK activity, whereas expression of RAC<sup>V12H40</sup> did not (Fig. 1, top). Thus, the activation of PAK by the RAC mutants is dependent on their ability to interact with PAK. To test for the ability of the RAC mutants to induce JNK activation, we cotransfected COS-1 cells with expression plasmids encoding RAC mutants and a plasmid encoding a FLAG-tagged version of JNK1. JNK activity was assayed with glutathione-S-transferase (GST) fused to c-Jun as the substrate (12). RAC<sup>V12H40</sup>, which did not bind to or activate PAK, also did not stimulate JNK activity (Fig. 1, bottom). The RAC<sup>V12L37</sup> mutant,

T. Joneson and D. Bar-Sagi, Department of Molecular Genetics and Microbiology, State University of New York, Stony Brook, NY 11794, USA.

M. McDonough and L. Van Aelst, Cold Spring Harbor Laboratory, 1 Bungtown Road, Cold Spring Harbor, NY 11724, USA.

\*These authors contributed equally to this work.

†To whom correspondence should be addressed.

which did interact with PAK, retained its ability to stimulate JNK activity. This result is not restricted to COS-1 cells; in rat embryo fibroblast (REF-52) cells, we observed stimulation of JNK activity by RAC<sup>V12L37</sup> but not by RAC<sup>V12H40</sup> (10). Thus, JNK activation by the RAC mutants is correlated with their ability to interact with PAK.

In fibroblast cells, RAC mediates growth factor-induced polymerization of actin, leading to the formation of membrane ruffles and lamellipodia (1). Expression plasmids encoding T7-tagged RAC mutants were microinjected into the nuclei of quiescent REF-52 cells, and induction of membrane ruffling was analyzed by staining with rhodamine-labeled phalloidin (13). Microinjection of RAC<sup>V12H40</sup> resulted in the induction of membrane ruffles to a similar extent as RAC<sup>V12</sup> (Fig. 2). No membrane ruffling was observed when RAC<sup>V12L37</sup> was microinjected. Immunofluorescence staining of the injected cells confirmed that all mutants were expressed to the same extent and displayed an overall similar subcellular distribution pattern (Fig. 2). Because all PAK isoforms share a similar sequence motif that mediates interaction with RAC1, our results suggest that PAK proteins do not mediate RAC-induced membrane ruffling and that activation of the JNK MAP kinase pathway is neither required nor sufficient for this cellular event. Our results suggest a role for POR1 in the induction of membrane ruffles. However, POR1 is unlikely to be the only RAC effector involved in membrane ruffling because we have previously shown that POR1 is necessary but not sufficient for the induction of membrane ruffling (8).

We have isolated a cDNA clone encoding a protein that interacts with RAC<sup>V12H40</sup> but not with RAC<sup>V12L37</sup> (Table 1). This clone corresponds to amino acids 812 through 1018 of the serine-threonine RHO-kinase (ROK $\alpha$ ), which is a RHO-binding protein (14) that phosphorylates and activates the myosin-binding subunit of myosin phosphatase (15). This results in an increase in myosin light chain phosphorylation and the consequent interaction of actin and myosin leading to stress fiber formation in non-muscle cells (15). The biological relevance of the interaction between RAC and ROK $\alpha$  to the effects of RAC on actin cytoskeleton remains to be defined.

RAC proteins play an important role in the regulation of cell growth (3–5). RAC<sup>V12</sup> induces DNA synthesis in Swiss 3T3 cells (5). A dominant negative form of RAC, RAC<sup>N17</sup> (N, asparagine), inhibits focus formation caused by oncogenic RAS in NIH 3T3 cells, and RAC<sup>V12</sup> synergizes strongly with RAF-CAAX (a c-RAF1 kinase targeted to the plasma membrane by a COOH-terminal lipid modification signal from H-RAS) in focus

formation assays (3). To examine the relative contribution of JNK and the morphology pathways to the mitogenic activity of RAC, we transfected RAC<sup>V12</sup>, RAC<sup>V12H40</sup>, and

RAC<sup>V12L37</sup> mutants together with RAF-CAAX into NIH 3T3 cells and scored them for the appearance of transformed foci after 14 days. Transfection of RAC<sup>V12</sup> or RAF-

**Table 1.** Interaction between RAC mutants and candidate RAC targets in the two-hybrid system. The candidate RAC targets fused to the GAL4 DNA-activating domain (GAD) were individually transformed into the yeast reporter strain L40 with LexA DNA binding domain (LBD) fusions containing RAC<sup>WT</sup> (wild-type Rac), indicated RAC mutants, and as a negative control, lamin. Transformants were grown in selective synthetic medium, and  $\beta$ -galactosidase ( $\beta$ -Gal) activity was assayed with *o*-nitrophenyl- $\beta$ -galactoside (8, 21); values are the mean  $\pm$  SD of triplicate determination. None of the RAC mutants bound to RAF, a RAS target, and all of them bound equally well to D4, a protein that has guanosine diphosphate dissociation inhibitor activity against CDC42 and RAC proteins in vitro (10).

LBD fusion	$\beta$ -Gal activity of GAD-fused RAC targets (Miller units)		
	PAK3	POR1	ROK $\alpha$
RAC <sup>WT</sup>	1.2 $\pm$ 1.1	42 $\pm$ 1.1	11 $\pm$ 2.3
RAC <sup>V12</sup>	62 $\pm$ 1.3	49 $\pm$ 1.9	57 $\pm$ 1.1
RAC <sup>V12H40</sup>	0.9 $\pm$ 1.3	22 $\pm$ 1.4	59 $\pm$ 1.1
RAC <sup>V12L37</sup>	59 $\pm$ 1.9	1.1 $\pm$ 0.9	0.8 $\pm$ 1.9
Lamin	0.9 $\pm$ 1.3	0.8 $\pm$ 0.9	0.7 $\pm$ 1.3

**Fig. 1.** Effects of RAC<sup>V12</sup>, RAC<sup>V12L37</sup>, and RAC<sup>V12H40</sup> on PAK and JNK activity. **(Top)** COS-1 cells were cotransfected with 10  $\mu$ g of Myc-tagged PAK1 and 10  $\mu$ g of the expression vector pCGT containing the indicated RAC mutants (22). Myc-tagged PAK1 was isolated from cell lysates by immunoprecipitation with monoclonal antibody (9E10) to Myc, and PAK kinase activity was measured in an immunocomplex kinase assay with MBP as a substrate. Radioactivity incorporated into MBP was visualized by autoradiography. Expression of PAK1 and RAC mutants was determined by protein immunoblot analysis with monoclonal antibodies to Myc and T7, respectively, and found to be similar in each sample. **(Bottom)** COS-1 cells were cotransfected with 10  $\mu$ g of FLAG-tagged JNK1 and 10  $\mu$ g of the expression vector pCGT containing the indicated RAC mutants. Treatment of cells with anisomycin (10  $\mu$ g/ml) for 20 min was used as a control. JNK kinase activity was measured by immunocomplex kinase assays with GST-Jun as the substrate and visualized by autoradiography. Expression of JNK1 and RAC mutants was determined by protein immunoblot analysis with monoclonal antibodies to FLAG M2 and T7, respectively, and found to be similar in each sample.

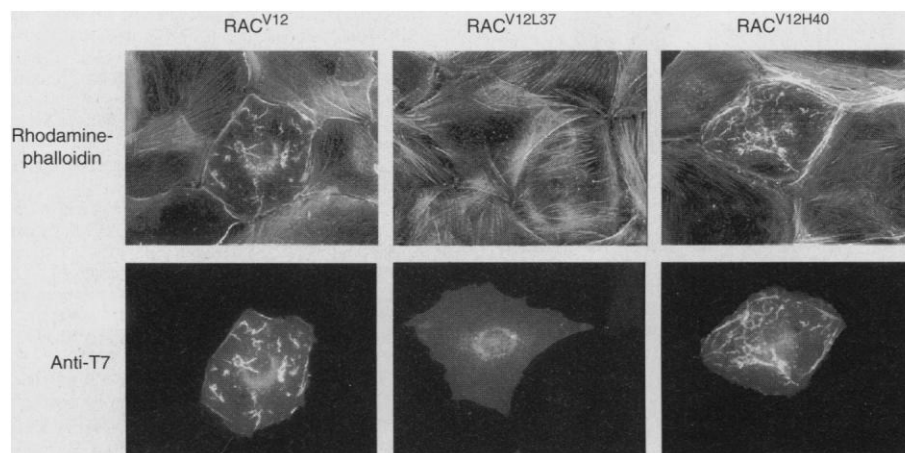
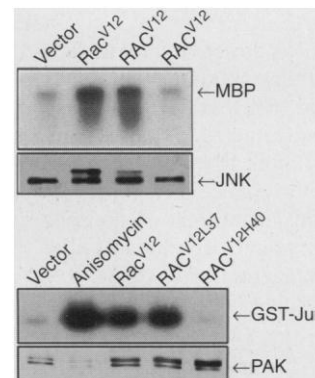


**Fig. 2.** Effects of RAC<sup>V12</sup>, RAC<sup>V12L37</sup>, and RAC<sup>V12H40</sup> on membrane ruffling. Quiescent REF-52 cells were microinjected with expression plasmids encoding the indicated RAC mutants (50  $\mu$ g/ml). Six hours after injection, cells were fixed and stained with rhodamine-labeled phalloidin to show membrane ruffles, which appear as bright areas of filamentous actin staining. Expression of the RAC mutants was confirmed by immunostaining with monoclonal antibodies to T7 (anti-T7) (73). Both the RAC<sup>V12</sup> and the RAC<sup>V12H40</sup> mutants were present in membrane ruffles.

CAAX alone (at a concentration of 100 ng per 10-cm dish) in NIH 3T3 cells produced very few transformed foci, whereas transfection of both together resulted in a synergistic enhancement in focus formation (Fig. 3). The RAC<sup>V12H40</sup> mutant, which is defective in JNK activation, did enhance focus formation, to a similar extent as did RAC<sup>V12</sup>, when cotransfected with RAF-CAAX. In contrast, the RAC<sup>V12L37</sup> mutant, which activates JNK, had no transforming activity. To exclude the possibility that RAF-CAAX might influence RAC<sup>V12H40</sup> ability to induce JNK activation, we cotransfected both RAF-CAAX and RAC<sup>V12H40</sup> together with a plasmid encoding a FLAG-tagged version of JNK1 and assayed JNK activity. The extent of JNK activation was similar to that of RAC<sup>V12H40</sup> alone (10). These results indicate that the pathway leading to JNK activation and the pathway through which RAC influences cell growth are mediated by distinct effectors of RAC.

Similar amino acid substitutions to those we analyzed in RAC1 have been made in RAS. RAS<sup>V12G37</sup> (G, glycine) activates JNK but is defective for stimulation of membrane ruffling and induction of DNA synthesis (10, 16), whereas RAS<sup>V12C40</sup> (C, cysteine) is defective for MAP kinase activation and stimulation of DNA synthesis but retained its ability to induce membrane ruffling (4, 16, 17). This might indicate the existence of common structural determinants that specify effector interactions of RAS and RAC. Alternatively, it could be that the effector or effectors that

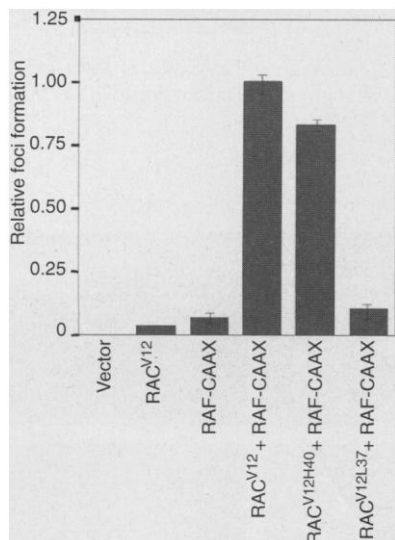


**Fig. 3.** Effects of the RAC mutants RAC<sup>V12</sup>, RAC<sup>V12H40</sup>, and RAC<sup>V12L37</sup> on focus-forming activities in NIH 3T3 cells. NIH 3T3 cells were transfected with the indicated plasmids (23). Relative foci formation was determined as the number of foci per number of G418-resistant colonies, then normalized to the focus formation frequency of RAC<sup>V12</sup> + RAF-CAAX, which was set at 1. The data shown are the mean  $\pm$  range of three dishes and are representative of three independent experiments.

mediate RAC- and RAS-induced membrane ruffling have common structural features.

The physiological function of JNK in mammalian cells is still unclear. Activation of JNK causes phosphorylation and activation of several transcription factors, including c-Jun, ATF-2, and Elk-1 (18). All of these transcription factors have been implicated in the expression of genes that regulate cell growth (19). Our results provide evidence that activation of the JNK MAP kinase pathway is not required for the growth-promoting activity of RAC. So far no RAC mutants have been isolated that separate the ability of RAC to induce membrane ruffling and to stimulate cell proliferation. Thus, it is possible that RAC-mediated pathways leading to actin polymerization and proliferation are interdependent.

## REFERENCES AND NOTES

- A. J. Ridley *et al.*, *Cell* **70**, 401 (1992).
- O. A. Coso *et al.*, *ibid.* **81**, 1137 (1995); A. Minden, A. Lin, F.-X. Xavier, A. Abo, M. Karin, *ibid.*, p. 1147; C. S. Hill, J. Wynne, R. Treisman, *ibid.*, p. 1159.
- R.-G. Qiu, J. Chen, D. Kim, F. McCormick, M. Symons, *Nature* **374**, 457 (1995); R. Khosravi-Far *et al.*, *Mol. Cell. Biol.* **15**, 6443 (1995).
- R. Khosravi-Far *et al.*, *Mol. Cell. Biol.* **16**, 3923 (1996).
- M. F. Olson, A. Ashworth, A. Hall, *Science* **269**, 1270 (1995).
- E. Manser *et al.*, *Nature* **367**, 40 (1994); U. G. Knaus S. Morris, H.-J. Dong, J. Chernoff, G. M. Bokoch, *Science* **269**, 221 (1995); S. Bagrodia *et al.*, *J. Biol. Chem.* **270**, 22731 (1995); G. A. Martin *et al.*, *EMBO J.* **14**, 1970 (1995).
- S. Zhang *et al.*, *J. Biol. Chem.* **270**, 23934 (1995); S. Bagrodia *et al.*, *ibid.*, p. 1; J. L. Brown *et al.*, *Curr. Biol.* **6**, 598 (1996).
- L. Van Aelst, T. Joneson, D. Bar-Sagi, *EMBO J.* **15**, 3778 (1996).
- For RAC mutant library construction and screening, full-length human RAC1 encoding a protein containing the activating G12V mutation (valine is substituted for glycine at position 12) was randomly mutagenized with PCR (20) and ligated in the vector pLexVJII (8) to create in-frame fusions with the LBD. Screening for mutations that affected binding of the LBD-RAC fusions to murine PAK3 or POR1 fused to the GAL4 activation domain vector pGAD1318 (8) was performed in the yeast strain L40 (8). Transformants from each screen, selected on synthetic media lacking leucine and tryptophan, were assayed for  $\beta$ -galactosidase activity on filters (21).
- T. Joneson, M. McDonough, D. Bar-Sagi, L. Van Aelst, unpublished results.
- For the PAK assay, COS-1 cells were cultured in Dulbecco's modified Eagle's medium (DMEM) supplemented with fetal bovine serum (FBS) (5%) and transfected by the standard calcium phosphate (CaPO<sub>4</sub>) method. For monitoring PAK activation, cells were cotransfected with 10  $\mu$ g of Myc-tagged PAK1 (from J. Chernoff) and 10  $\mu$ g of the expression vector pCGT containing either no insert, RAC<sup>V12</sup>, RAC<sup>V12H40</sup>, or RAC<sup>V12L37</sup>. After a 12-hour incubation with the DNA-CaPO<sub>4</sub> precipitates, cells were incubated in media containing FBS (5%) for 6 hours and then incubated for 12 hours in serum-free medium. Cells were lysed in lysis buffer [10 mM Hepes (pH 7.5), 10% glycerol, 150 mM NaCl, 1 mM Na<sub>2</sub>VO<sub>4</sub>, 0.6% Triton X-100, 50 mM NaF, 1 mM okadaic acid, 1 mM benzamide, 1 mM phenylethylsulfonamide, leupeptin (10  $\mu$ g/ml), aprotinin (10  $\mu$ g/ml)]. Myc-tagged PAK1 was immunoprecipitated with 5  $\mu$ g of Myc monoclonal antibody 9E10. Immune complexes were collected by binding to protein G-Sepharose, washed extensively with lysis buffer, then incubated for 30 min at 37°C in kinase assay buffer [20 mM Hepes (pH 7.6), 20 mM MgCl<sub>2</sub>, 20 mM  $\beta$ -glycerol phosphate, 0.1 mM Na<sub>3</sub>VO<sub>4</sub>, 2 mM dithiothreitol, 20  $\mu$ M adenosine triphosphate (ATP)] and 10  $\mu$ Ci of [ $\gamma$ -<sup>32</sup>P]ATP with MBP (0.2 mg/ml) as substrate. The reaction products were analyzed by SDS-polyacrylamide gel electrophoresis and visualized by autoradiography.
- JNK activity in vitro was measured as described in (11) with the following exceptions: Cells were transfected with 10  $\mu$ g of FLAG-tagged JNK1 (gift from R. Cerione). After cell lysis, JNK1 was immunoprecipitated with 5  $\mu$ g of monoclonal antibody to FLAG M2 (Eastman Kodak). Immune complexes were collected by binding them to protein G-Sepharose and then incubated with GST fused to the NH<sub>2</sub>-terminal of c-Jun (3  $\mu$ g per reaction) in kinase assay buffer.
- For the microinjection assay, REF-52 cells were plated onto glass cover slips and cultured in DMEM supplemented with FBS (10%). The cells were grown to confluence, then placed in DMEM with 0.5% FBS for 24 hours before microinjection. A plasmid mixture containing indicated plasmids in microinjection buffer [50 mM Hepes (pH 7.2), 100 mM KCl, and 5 mM NaHPO<sub>4</sub>] was microinjected into cell nuclei. For monitoring membrane ruffles and subcellular localization, cells on cover slips were fixed in 3.7% formaldehyde in phosphate-buffered saline (PBS) for 1 hour at room temperature and then permeabilized with 0.1% Triton X-100 in PBS for 3 min at room temperature. The cover slips were incubated for 1 hour at 37°C with mouse antibody to T7 epitope (Novogen) in PBS containing albumin (2 mg/ml) and then with a mixture of fluorescein-conjugated goat antibody to mouse immunoglobulin G and rhodamine-labeled phalloidin (0.01 mg/ml) (Molecular Probes). The cells were photographed with a Zeiss Axiophot fluorescence microscope.
- T. L. Leung, E. Manser, L. Tan, L. Lim, *J. Biol. Chem.* **270**, 29051 (1995); T. Matsui *et al.*, *EMBO J.* **15**, 2208 (1996).
- K. Kimura *et al.*, *Science* **273**, 245 (1996).
- L. Van Aelst, M. A. White, M. H. Wigler, *Cold Spring Harbor Symp. Quant. Biol.* **59**, 181 (1994); M. W. White *et al.*, *Cell* **80**, 533 (1995).
- T. Joneson, M. A. White, M. H. Wigler, D. Bar-Sagi, *Science* **271**, 810 (1996).
- M. Hibi *et al.*, *Genes Dev.* **7**, 2135 (1993); B. Derjard *et al.*, *Cell* **76**, 1025 (1994); S. Gupta, D. Campbell, B. Derjard, R. J. Davis, *Science* **267**, 389 (1995); H. A.-M. Abdel-Hafiz *et al.*, *Mol. Endocrinol.* **6**, 2079 (1992); A. J. Whitmarsh *et al.*, *Science* **269**, 403 (1995); H. Gille *et al.*, *Curr. Biol.* **5**, 1191 (1995).
- M. Karin and T. Hunter, *Curr. Biol.* **5**, 747 (1995).
- Y. Zhou, X. Zhang, R. H. Ebright, *Nucleic Acids Res.* **19**, 6052 (1991).
- L. Van Aelst *et al.*, *Proc. Natl. Acad. Sci. U.S.A.* **90**, 6213 (1993).
- Plasmid pCGT, which is derived from pCGN with a replacement of the Lerner epitope by the T7 epitope (8), was used as a mammalian expression vector to express the various RAC mutants. pCGT RAC<sup>V12</sup> contains full-length RAC<sup>V12</sup> inserted as a Bam HI-Sal I fragment into pCGT. pCGT RAC<sup>V12H40</sup> and pCGT RAC<sup>V12L37</sup> were constructed by replacing the Nsi I-Sal I fragment of pCGT RAC<sup>V12</sup> by the one of LBD RAC<sup>V12H40</sup> and LBD RAC<sup>V12L37</sup>, respectively. RAF-CAAX was cloned in the mammalian expression vector pcDNA3 (Invitrogen) and was a gift from J. Stolarov. pGAD-PAK3 was obtained by subcloning a Bam HI fragment of pcDNA3-PAK3 (gift from S. Bagrodia and R. Cerione) into pGAD1318.
- NIH 3T3 cells were transfected by the CaPO<sub>4</sub> method (16) with the indicated expression plasmids (100 ng per 10-cm dish for each plasmid). Transfected cells were grown in media containing calf serum (5%) for 14 days, then fixed in 10% formaldehyde and stained with Giemsa. Foci of transformed cells appear as diffuse, darkly staining spots.
- We thank R. Packer for technical help and J. Stolarov, S. Bagrodia, R. Cerione, and J. Chernoff for providing plasmids. Supported by Cold Spring Harbor Laboratory interim research support funds to L.V.A. and NIH grant CA55360 to D.B.-S.

30 July 1996; accepted 3 October 1996